Defect-mediated turbulence in the Belousov-Zhabotinsky reaction

Chun Qiao,[1] Hongli Wang,[1,2,3,*] and Qi Ouyang[1,2,3,*]
[1]*State Key Laboratory for Mesoscopic Physics, Department of Physics, Peking University, Beijing 100871, China*
[2]*The Beijing-Hong Kong-Singapore Joint Center for Nonlinear and Complex Systems, Peking University, Beijing 100871, China*
[3]*Center for Theoretical Biology, Peking University, Beijing 100871, China*
(Received 14 July 2008; revised manuscript received 13 November 2008; published 21 January 2009)

Statistical properties of topological defects in defect-mediated turbulence due to the Doppler instability are examined experimentally in the Belousov-Zhabotinsky reaction. By applying the phase space reconstruction approach, processes of defect creation, annihilation, and defect movement are analyzed. The defect dynamics can be well interpreted within the framework of stochastic Markovian process. In contrast to previous studies that made direct measure of the gain and loss rates, which is practically difficult, we demonstrate that the rates can be obtained directly from the analysis of the time series of defects, and the shape of the probability distribution function can be reproduced in a simple way.

DOI: 10.1103/PhysRevE.79.016212 PACS number(s): 05.45.Jn, 05.40.−a, 82.40.Ck

Topological defects caused by symmetry breaking are abundant in nature. Examples in physics include screw dislocations in crystal [1], fluxon-antifluxon pairs in Josephson transmission line [2], and magnetic monopoles in cosmology [3]. There are also examples in chemistry and hydrodynamics, from defect-mediated turbulence in the Belousov-Zhabotinsky (BZ) reaction [4] and electrochemical reactions [5], to vortices in fluids [6] and convective systems [7]. In spatially extended systems, the presence of defects often dominates spatiotemporal chaos. Although pattern formation has been intensively studied in the past decades, defect-mediated turbulence is still poorly understood and remains a challenge in this field. To characterize the disordered states featured by defects, recent attention has been paid to the statistical properties of topological defects. Theoretical work was first carried out with the complex Ginzburg-Landau equation (CGLE) [8], where the probability distribution function (PDF) for the number of defects was found to be the squared-Poisson distribution. Statistical properties of defects were also analyzed numerically in a FitzHugh-Nagumo-type system [9], in the chemical Willamowski-Rössler reaction-diffusion model [10], and in a model of forced catalytic CO oxidation [11]. Experimental studies of defect statistics are still rare and were mainly reported from electroconvection in liquid crystals [12] and catalytic surface reactions [13].

The BZ reaction that takes place in the spatial open reactor has been a prototype model system for the study of pattern formation in reaction-diffusion systems [4]. As one of the most common spatiotemporal patterns in oscillatory and excitable media, spiral waves have been extensively studied in the BZ system. The spiral waves were reported to lose their stabilities through scenarios such as the Doppler instability [14] and the Eckhaus instability [15], and generate chemical turbulence dominated by spiral vortices. While the defect-mediated turbulence in the BZ reaction has been observed for many years, its dynamics has never been studied in detail.

*Authors to whom correspondence should be addressed; hlwang@pku.edu.cn, qi@pku.edu.cn

In this paper, the statistical properties of defects in the defect-mediated turbulence are examined in the reaction-diffusion system. Using our experimental setup of the spatial open reactor, image sequences of defect-mediated turbulence due to the Doppler instability in the BZ reaction are recorded. The Doppler instability is caused by the nonsupport of excessively frequent excitation at local regions due to the Doppler effect of the nonlinear waves and tips number can increase quickly from one to many. The images are analyzed in combination with sequences generated by reconstructing the phase space of the local dynamics. The defect dynamics is found to be well interpreted within the framework of a stochastic Markovian process. In contrast to previous studies that made direct measure of the gain and loss rates, we show that the rates of defect creation, decay, and entering and leaving the observation area can be obtained directly from the analysis of the time series of defects. The shape of the probability distribution function (PDF) can then be reproduced in a simple way.

Experiment. The BZ experiment is carried out in a spatial open reactor similar to that used in previous studies [16]. The reaction medium is a 0.4-mm-thick porous glass, 22 mm in diameter, sandwiched by two continuously fed stirred tank reactors (CSTRs) (I) and (II), and the spatial open reactor is placed in a constant temperature device. A ferroin-catalyzed BZ reaction is used. The two-dimensional (2D) projection of the patterns is registered by a CCD camera. The data are recorded in a computer via a frame grabber.

Different chemical reactants are fed into CSTRs (I) and (II); they diffuse into the reaction medium and form a patterned layer that supports spiral waves inside the medium. Under our experimental conditions, the patterned layer is thin and can be considered as a 2D system [17]. In the experiments, we choose $[H_2SO_4]^{I}$ as the control parameter, varying from $0.33M$ to $0.40M$ with precision $0.0075M$. Other parameters are kept fixed: $[NaBrO_3]^{I,II}=0.6M$, $[CH_2(COOH)_2]^{I}=0.1M$, $[KBr]^{I}=30$ mM, and $[Ferroin]^{II}=0.15$ mM. The reaction temperature is 25 ± 0.2 °C.

We begin the experiments at low $[H_2SO_4]^{I}$ with only one meandering spiral in the medium, which has a cycloid spiral tip trajectory [19]. When we increase the control parameter to $0.3450M$, the meandering spiral begins to break up due to

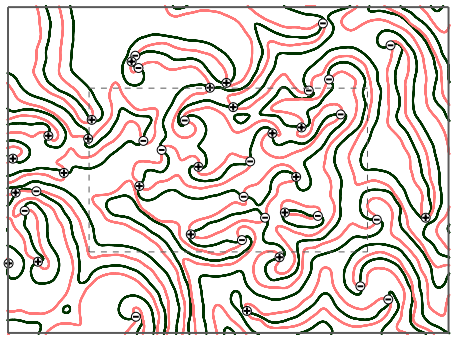

FIG. 1. (Color online) The isoline contours and the distinguished topological positive (with charge $m_{\text{top}}=1$) and negative (with $m_{\text{top}}=-1$) defects denoted by "+" and "−," respectively. $[H_2SO_4]^I=0.3750M$.

the Doppler instability and defect-mediated turbulence will dominate the system [17]. If one increases $[H_2SO_4]^I$ further beyond the transition point, the patterns become more turbulent. We record movies of the turbulent pattern under different $[H_2SO_4]^I$ for latter processing [18]. The time interval Δt between two adjacent frames is always 0.4 s and the movies typically consist of more than 10 000 images.

Results. A defect in the turbulent pattern corresponds to a local position where the oscillation amplitude is zero and the phase is undefined. It is characterized by its topological charge defined by $\frac{1}{2\pi}\oint \nabla\phi(r,t)dl=m_{\text{top}}$, where $\phi(r,t)$ is the local phase and the integral is calculated along a closed curve surrounding the defect, and the charge m_{top} takes typically +1 or −1. As only one image sequence is recorded for the time evolution of turbulence in our experiments, we generate another image sequence $v(\mathbf{r},t_i)$ from the original image intensity $u(\mathbf{r},t_i)$ by reconstructing the phase space of the local dynamics with time-delayed coordinates, i.e., $v(\mathbf{r},t_i)\equiv u(\mathbf{r},t_i-\tau)$, with $\tau=3.2$ s. The location of a defect can then be identified where the isoline contours of u and v fields intersect. Figure 1 demonstrates the contours and the distinguished defects marked with "+" or "−" for their topological charges +1 or −1 [18].

To examine the dynamics of topological defects, we concentrate on the central part of the images as marked in Fig. 1, which is a 6.9×4.1 mm area. The defects are created and annihilated irregularly in pairs, and also enter or leave incidentally the area of observation. The number of defects in the area as a function of time $n(t_i)$ is found to be a random fluctuation around its mean value. Figure 2 depicts PDFs for the number of defects with different value of $[H_2SO_4]^I$ ("○" in Fig. 2). We see that the experimental distributions are always lower than the Poisson distribution. To obtain the gain and loss rates of defects, we apply a computer-automated procedure to distinguish the elementary events: Creations and annihilations of defect in pairs, where the number of defects is increased or decreased by 2; and the boundary crossings when defects are entering or leaving the observation area, where the defect number is increased or reduced by 1. The procedure is based on a nearest-neighbor tracking scheme, and has been checked manually to ensure its accuracy. The rates for the elementary events are calculated by counting the number of current defects and those

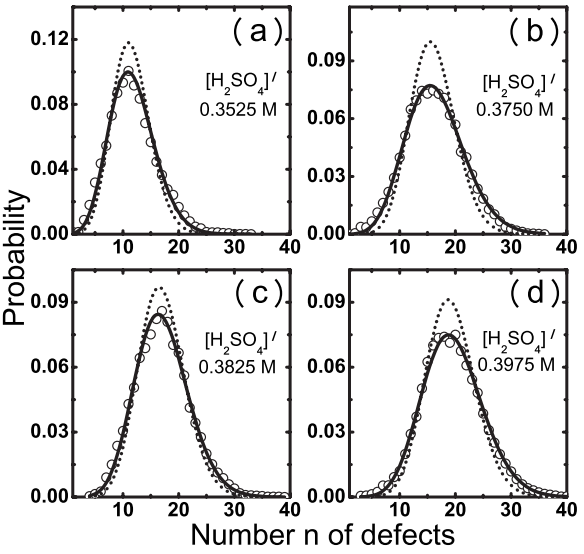

FIG. 2. The probability distributions of defect numbers n under different concentration $[H_2SO_4]^I$: (a) $0.3525M$; (b) $0.3750M$; (c) $0.3825M$; (d) $0.3975M$. Open circles are for experimental results, dotted curves are Poisson distributions, and black curves are for theoretical predictions.

that are created, annihilated, entering, and leaving in a subsequent time unit Δt and are then averaged over the recorded experimental time. An example of the gain and loss rates as functions of the defect number are shown in Fig. 3. The creation, the entering, and the leaving show linear dependence on the number of defects n, while the annihilation rate is quadratic. As the concentration $[H_2SO_4]^I$ is varied, the linear dependence of creation-entering-leaving and quadratic dependence of annihilation on defect numbers are not different. The rates for defects entering and leaving the observa-

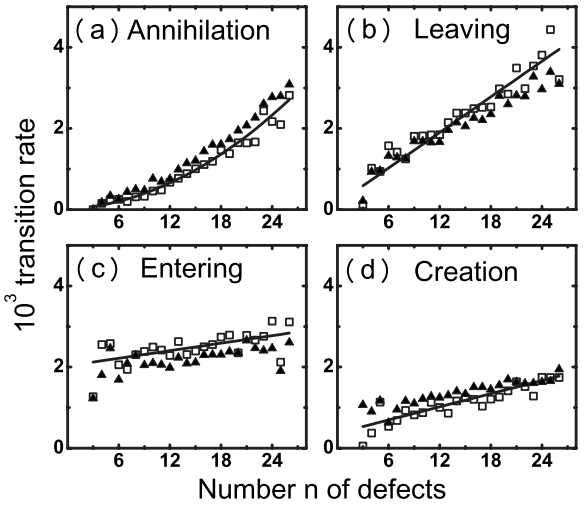

FIG. 3. Gain and loss rates obtained from direct experimental measurements ("▲") and from the transition matrix $\mathbf{S}(\frac{\Delta t}{D})$ ("□") with $D=100$. The full lines are fittings of the data. (a) Annihilation, fitted with $A(n)=3.56\times10^{-6}n^2+4.15\times10^{-6}n$; (b) leaving, fitted with $L(n)=1.46\times10^{-4}n$; (c) entering, fitted with $E(n)=3.10\times10^{-5}n+2.00\times10^{-3}$; (d) creation, fitted with $C(n)=5.40\times10^{-5}n+3.18\times10^{-4}$. $[H_2SO_4]^I=0.3750M$.

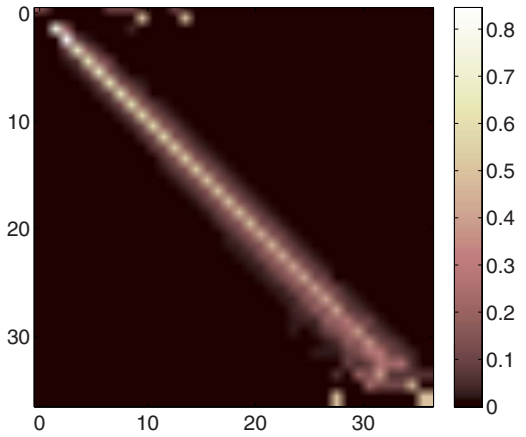

FIG. 4. (Color online) Graphic representation of the transition matrix $\mathbf{S}(\Delta t)$ generated with $[H_2SO_4]^I=0.3750M$. The transition rates concentrate on the matrix diagonal, and elements far from the diagonal take very small values.

tion area increase linearly when there are more defects present in the system, implying a growing mobility and instability of the defects. The creation rate grows also linearly with defects in the system, suggesting that besides a constant creation rate, the instability of the system grows when more defects are present in the system and defects are created with an additional rate proportional to defect numbers.

The experimental PDFs for the number of defects can be explained with a simple probabilistic model by assuming that the defects are statistically independent and the gain and loss of defects in the observed area follow a discrete stochastic Markovian transition process. In previous studies, the shape of the PDF was always interpreted on the base of the observed gain and loss rates. In the following, we demonstrate that the experimental data including both the gain or loss rates and the PDFs can be explained directly from the time series of defect number $n(t_i)$.

In the framework of a Markovian transition process, the transition rate $S(\Delta t)_{k,j}$ for a current state having j defects to jump to a state with k defects can be obtained by checking every jumping in the time interval Δt, i.e., from $n(t_i)$ to $n(t_{i+1})$, for its occurrence frequency in the time series $n(t_i)$. The rate $S(\Delta t)_{k,j}$ can then be readily obtained and normalized by $\Sigma_k S(\Delta t)_{k,j}=1$. Figure 4 depicts a graphic representation of the transition matrix with concentration $[H_2SO_4]^I=0.3750M$. Most of the matrix elements are trivial and the nonzero elements concentrate along the neighborhood of the diagonal. The master equation for the PDF $P(k,t)$ having k defects at time t takes the following form:

$$P(k,t+\Delta t)=\sum_{j=0}^{+\infty} S(\Delta t)_{k,j}P(j,t). \tag{1}$$

In the stationary state of detailed balance, the probability distribution $P(k)$ for the number of defects satisfies the master equation, $\mathbf{S}(\Delta t)\mathbf{P}=\mathbf{P}$. In practice, the number of defects is limited in a certain range $[0,N]$, and the stationary probability $P(k)$ satisfies the linear algebra equation,

$$\begin{pmatrix} S_{00}S_{01}\cdots S_{0N} \\ S_{10}S_{11}\cdots S_{1N} \\ \vdots \\ S_{N0}S_{N1}\cdots S_{NN} \end{pmatrix}_{(\Delta t)} \begin{pmatrix} P(0) \\ P(1) \\ \vdots \\ P(N) \end{pmatrix} = \begin{pmatrix} P(0) \\ P(1) \\ \vdots \\ P(N) \end{pmatrix}. \tag{2}$$

With the transition matrix $\mathbf{S}$ determined from the time series of defect number $n(t_i)$, the stationary probability $P(k)$ obtained from the above equation is in exact agreement with the experimental distributions (not shown). The underlying dynamics of defect is thus a well-defined Markovian transition process.

The transition rate $\mathbf{S}(\Delta t)_{k,j}$ is a function of Δt, which is the time interval between two adjacent frames of the movies. $\Delta t=0.4$ s, which was adopted in our experiments, is not very small as compared to 15 s oscillation period of the media. If Δt is reduced by D folds to $\frac{\Delta t}{D}$, the new transition matrix $\mathbf{S}(\frac{\Delta t}{D})$ satisfies the relation,

$$\mathbf{S}(\Delta t)=\underbrace{\mathbf{S}\left(\frac{\Delta t}{D}\right)\cdots\mathbf{S}\left(\frac{\Delta t}{D}\right)}_{D}. \tag{3}$$

Thus $\mathbf{S}(\frac{\Delta t}{D})$ can be obtained by computing the principal Dth root of $\mathbf{S}(\Delta t)$ [23]. We find that as D is large enough, the newly calculated matrix $\mathbf{S}(\frac{\Delta t}{D})$ contains only nonzero elements of $S(\frac{\Delta t}{D})_{k,j}$ with $k=j-2,j-1,j,j+1,j+2$.

The transition rate $S(\Delta t)_{k,j}$ has been contributed in combination by the underlying elementary steps of defect creation, decay, entering and leaving, and their concurrences in the time interval Δt. For instance, in a jump from j to $j+2$, a defect-creation event and a concurrence of two entering events would both contribute to $S(\Delta t)_{j+2,j}$; a jump from j to $j+1$ would be fulfilled through simply an entering event or a combination of a creation and a leaving event, etc. When Δt is decreased, the chance of concurrence of these elementary processes is expected to be reduced significantly. The transition rate would be the most principally contributed by an individual elementary step. In fact, the contribution to the transition rate from an elementary step is a first-order infinitesimal of the time interval, while the contributions from their concurrences are the second- and even higher-order infinitesimals. As the time interval is sufficiently small, the transition rate $S(\Delta t)_{k,j}$ could be considered as being solely contributed by one of the four elementary steps. Therefore, the nonzero elements $S(\frac{\Delta t}{D})_{k,j}$ obtained when D is sufficiently large correspond, respectively, to the rates for the four elementary processes: $S(\frac{\Delta t}{D})_{j+2,j}$ is the rate for defect creation $C(j)$; $S(\frac{\Delta t}{D})_{j-2,j}$ is the rate for defect annihilation $A(j)$, $S(\frac{\Delta t}{D})_{j+1,j}$ and $S(\frac{\Delta t}{D})_{j-1,j}$ are the rates $E(j)$ and $L(j)$ for a defect to enter and to leave the observation area, respectively. In fact, as D grows to infinity, the nonzero elements in $\mathbf{S}(\frac{\Delta t}{D})$ become quickly proportional to $\Delta t/D$, the gain and loss rates can be readily obtained. While how fine the time resolution $\Delta t/D$ should be could not be deduced *a priori* in order to resolve the gain and loss rates, in practice we find that the rates thus obtained converge very quickly as D grows. The rates can be well generated with a D larger than 50.

Figure 3 demonstrates the transition rates obtained with the time interval $\frac{\Delta t}{D}=0.004$ s (with $D=100$). They are in agreement with the rates determined by checking directly the image sequence. The rates are found to be best fitted with simple functions: $A(n)=a_2n^2+a_1n$, $L(n)=l_1n$, $E(n)=e_1n+e_0$, and $C(n)=c_1n+c_0$. With these fittings, we can reconstruct the transition matrix $\mathbf{S}_f(\frac{\Delta t}{D})$ which is a fitting for $\mathbf{S}(\frac{\Delta t}{D})$. The stationary probability distributions $P(n)$ obtained by solving $\mathbf{S}_f(\frac{\Delta t}{D})\mathbf{P}=\mathbf{P}$ turn out to agree very well with the experimental data, as has been depicted in Fig. 2.

Conclusion and Discussion. We have studied the statistical properties of topological defects in the chemical turbulence caused by the Doppler instability of spiral waves in the BZ reaction. Images recorded in our experiments and the dynamics of defects have been analyzed by reconstructing a two-dimensional phase space for the local dynamics. We have demonstrated that statistical properties of the defects can be well explained within the framework of a stochastic Markovian process. In addition to the direct measuring of the gain and loss rates of the defects, which is practically a difficult approach, we have shown that the rates can be alternatively and conveniently generated from the time series of defect number $n(t_i)$ when the transition matrix $\mathbf{S}(\Delta t)$ goes to the limit $\Delta t\rightarrow 0$.

The gain and loss rates could be regarded as a measure of the instability for the turbulence. A faster gain or loss rate implies a more intensive instability in the turbulence. The rates are also different from different systems, implying characteristic instabilities for turbulence in a specific system. The defect annihilation rate in the BZ reaction we report here is a combined quadratic and linear dependence on the defect number n. This is identical with the results reported earlier from the catalytic surface reaction [20] and CGLE influenced by noise [21], but deviates from the result of Gil *et al.* [8] and the case of electroconvection in liquid crystals [12] where the annihilation rate was previously found to be proportional to the square of n. We find that the creation, entering, and leaving of defects increase linearly with n. This is in contrast to the catalytic surface reaction [20] where the creation and the entering rates are constant and the leaving of defects is a linear function of n. In the BZ reaction, the rates for defects entering and leaving the observation area increase linearly when there are more defects present in the system, implying a growing mobility and instability of the defects. A quadratic polynomial with an additional linear term implies that the instability of the system is increased by an amount compared to the simple quadratic case. No matter the different gain and loss rates of defects in different systems, statistical properties of defects have been uniformly explained in the framework of a Markovian transition process. The statistical description of defect chaos was recently extended to the Gray-Scott system where the disordered states are dominated by the random creation and decay of self-replicating spots [22]. Combined, the findings in defect chaos and the turbulence dominated by other types of entities, we suggest that the Markovian transition process provides a potentially universal description of statistical properties in spatiotemporal chaos.

This work was supported by the Natural Science Foundation of China (Grant No. 10774008) and National Basic Research Program of China (973 Program) (Grants No. 2006CB910706 and No. 2007CB814800).

[1] A. Redinger, O. Ricken, P. Kuhn, A. Rätz, A. Voigt, J. Krug, and T. Michely, Phys. Rev. Lett. **100**, 035506 (2008).
[2] K. Nakajima, H. Mizusawa, Y. Sawada, H. Akoh, and S. Takada, Phys. Rev. Lett. **65**, 1667 (1990).
[3] P. Bhattacharjee and G. Sigl, Phys. Rev. D **51**, 4079 (1995).
[4] Q. Ouyang and J. M. Flesselles, Nature (London) **379**, 143 (1996).
[5] S. Jakubith, H. H. Rotermund, W. Engel, A. von Oertzen, and G. Ertl, Phys. Rev. Lett. **65**, 3013 (1990).
[6] G. N. Stratopoulos and T. N. Tomaras, Phys. Rev. B **54**, 12493 (1996).
[7] R. E. Ecke and Y. Hu, Physica A **239**, 174 (1997).
[8] L. Gil, J. Lega, and J. L. Meunier, Phys. Rev. A **41**, 1138 (1990).
[9] M. Hildebrand, M. Bär, and M. Eiswirth, Phys. Rev. Lett. **75**, 1503 (1995).
[10] J. Davidsen and R. Kapral, Phys. Rev. Lett. **91**, 058303 (2003).
[11] J. Davidsen, A. Mikhailov, and R. Kapral, Phys. Rev. E **72**, 046214 (2005).
[12] K. E. Daniels and E. Bodenschatz, Phys. Rev. Lett. **88**, 034501 (2002).
[13] H. Varela, C. Beta, A. Bonnefont, and K. Krischer, Phys. Rev. Lett. **94**, 174104 (2005).
[14] Q. Ouyang, H. L. Swinney, and G. Li, Phys. Rev. Lett. **84**, 1047 (2000).
[15] L. Q. Zhou and Q. Ouyang, Phys. Rev. Lett. **85**, 1650 (2000).
[16] C. X. Zhang, H. M. Liao, and Q. Ouyang, J. Phys. Chem. B **110**, 7508 (2006).
[17] Q. Ouyang, H. L. Swinney, and G. Li, Phys. Rev. Lett. **84**, 1047 (2000).
[18] See EPAPS Document No. E-PLEEE8-79-081901 for the turbulence and for the contour and defects. For more information on EPAPS, see http://www.aip.org/pubservs/epaps.html.
[19] G. Li, Q. Ouyang, V. Petrov, and H. L. Swinney, Phys. Rev. Lett. **77**, 2105 (1996).
[20] C. Beta, A. S. Mikhailov, H. H. Rotermund, and G. Ertl, Europhys. Lett. **75**, 868 (2006).
[21] H. Wang, Phys. Rev. Lett. **93**, 154101 (2004).
[22] H. Wang and Q. Ouyang, Phys. Rev. Lett. **99**, 214102 (2007).
[23] L. Shieh, Y. T. Tsay, and R. E. Yates, IEEE Trans. Autom. Control **30**, 606 (1985).